J Appl Electrochem (2009) 39:1153–1156
DOI 10.1007/s10800-008-9772-3

SHORT COMMUNICATION

# Electro-oxidation of ethanol on PtSn/$CeO_2$–C electrocatalyst

**Almir Oliveira Neto · Marcelo Linardi · Daniela M. dos Anjos · Germano Tremiliosi-Filho · Estevam V. Spinacé**

Received: 20 August 2008 / Accepted: 23 December 2008 / Published online: 6 January 2009


**Abstract** PtSn/$CeO_2$–C electrocatalyst was prepared in a single step by an alcohol-reduction process using ethylene glycol as solvent and reducing agent and $CeO_2$ (15 wt%) and Vulcan XC72 (85 wt%) as supports. The performance for ethanol oxidation was investigated by cyclic voltammetry and in situ FTIR spectroscopy. The electrocatalytic activity of the PtSn/$CeO_2$–C electrocatalyst was higher than that of the PtSn/C electrocatalyst. FTIR studies for ethanol oxidation on PtSn/C electrocatalyst showed that acetaldehyde and acetic acid were the principal products formed, while on PtSn/$CeO_2$–C electrocatalyst the principal products formed were $CO_2$ and acetic acid.

**Keywords** PtSn/$CeO_2$–C · Alcohol-reduction process · Ethanol oxidation · Fuel cell · FTIR spectroscopy

## 1 Introduction

Direct Alcohol Fuel Cells (DAFCs) are attractive as power sources for mobile and portable applications [1, 2]. Ethanol offers an attractive alternative as fuel because it is produced in large quantities from biomass and is much less toxic than methanol. On the other hand, its complete oxidation to $CO_2$ and water is more difficult than that of methanol due to the difficulties in C–C bond breaking and to the formation of CO-intermediates that poison the platinum anode catalysts [3–5]. Thus, its complete oxidation remains a great challenge and the principal products formed are acetaldehyde and/or acetic acid [6, 7]. Thus, new catalyst materials and new catalyst preparation method developments have been one of the major topics studied concerning the electro-oxidation of ethanol [4, 8]. PtSn/C electrocatalyts are claimed to be more active than PtRu/C electrocatalysts for ethanol electro-oxidation and their performance depends greatly on the preparation procedure and Pt:Sn atomic ratio [9–11]. PtSn/C electrocatalysts prepared by an alcohol-reduction process, where Pt was found as face-centred cubic (fcc) and Sn as a $SnO_2$ phase, were very active for methanol and ethanol oxidation [12]. Mann et al. [13] found that a nanoparticulate catalyst containing Pt and $SnO_2$ allowed the partial conversion of ethanol to $CO_2$ and water and the elevation of the operating temperature of direct ethanol fuel cell (DEFC) to 130 °C facilitated the production of $CO_2$ and provided an improvement of current–voltage response.

Recently, we prepared PtSn/$CeO_2$–C electrocatalysts by an alcohol-reduction process in a single step [14], substituting part of the carbon support by $CeO_2$. The material obtained was more active for ethanol oxidation than the analogous PtSn/C catalyst. In this work, the electrochemical oxidation of ethanol on PtSn/$CeO_2$–C electrocatalyst was investigated by in situ FTIR spectroscopy to obtain information about intermediates and reaction products.

## 2 Experimental

PtSn/C and PtSn/$CeO_2$–C (Pt:Sn atomic ratio 50:50) electrocatalysts were prepared with metal loading of 20 wt%

A. O. Neto (✉) · M. Linardi · E. V. Spinacé (✉)
Instituto de Pesquisas Energéticas e Nucleares - IPEN-CNEN/SP, Cidade Universitária, Av. Prof. Lineu Prestes, 2242, CEP 05508-900 Sao Paulo, SP, Brazil
e-mail: aolivei@ipen.br

E. V. Spinacé
e-mail: espinace@ipen.br

D. M. dos Anjos · G. Tremiliosi-Filho
Instituto de Química de São Carlos, Universidade de São Paulo, Caixa Postal 780, CEP 13560-970 Sao Carlos, SP, Brazil

using $H_2PtCl_6 \cdot H_2O$ (Aldrich) and $SnCl_2 \cdot 2H_2O$(Aldrich) as metal sources, ethylene glycol (Merck) as solvent and reducing agent and $CeO_2$ (15 wt%) and carbon Vulcan XC72 (85 wt%) as support [12, 15, 16]. In a typical procedure the metal sources were dissolved in ethylene glycol/water (75/25, v/v) and the supports were added. The resulting mixtures were treated in an ultrasonic bath and were refluxed for 3 h under open atmosphere. The mixtures were filtered and the solid was washed with water and dried at 70 °C for 2 h.

Pt:Sn atomic ratios were obtained by EDAX analysis using a scanning electron microscope Philips XL30 with a 20 keV electron beam and equipped with EDAX DX-4 microanalyser. XRD analyses were performed using a Rigaku diffractometer model Multiflex with a CuK$\alpha$ radiation source.

The electrochemical activity of the electrocatalysts was evaluated in 0.5 mol $L^{-1}$ $H_2SO_4$ solution containing 0.5 mol $L^{-1}$ of ethanol by cyclic voltammetry in a three-electrode cell using a Voltalab Potentiostat PGZ 420. A Reversible Hydrogen Electrode (RHE) was used as reference and vitreous carbon as auxiliary electrode.

The spectroelectrochemical measurements were carried out in a Fourier transform infrared spectrometer Nicolet Nexus 670 with a MCT detector. The electrochemical cell was fitted with a 60° prismatic $CaF_2$. Reflectivities were recorded after applying potentials steps of 50 mV toward more positive potentials (from 0.050 to 1.000 V *vs* RHE) in 0.5 mol $L^{-1}$ $H_2SO_4$ solution containing 0.5 mol $L^{-1}$ of ethanol. Each spectrum was the resulted from the co-addition of 128 interferograms. Spectra were calculated as $-\Delta A = \Delta R/R = (R_{E2} - R_{E1})/R_{E1}$ where the "reference" spectrum, $R_{E1}$, was that recorded at the initial potential at 0.050 V vs RHE. For the calculations, $E_2 > E_1$, so that, a positive absorption band indicates the consumption of species and a negative absorption band means the production of species.

## 3 Results and discussion

As already published for PtSn/C and PtSn/$CeO_2$–C electrocatalysts [14], the Pt:Sn atomic ratios obtained by EDAX were very similar to the nominal ones and from XRD measurements it was observed that Pt (fcc), $SnO_2$ and $CeO_2$ coexist in PtSn/$CeO_2$–C electrocatalyst. The average crystallite sizes of Pt(fcc) phase present in PtSn/C and PtSn/$CeO_2$–C electrocatalysts were very similar (about 2.5 nm) [14].

Figure 1 shows the cyclic voltammograms (CV) of PtSn/C and PtSn/$CeO_2$–C electrocatalysts in acid solution. The cyclic voltammogram for the PtSn/C electrocatalyst do not show a well-defined hydrogen adsorption–desorption region (0.05–0.4 V). The cathodic scan showed one small peak at about 0.8 V that may be attributed to the reduction of oxide species. PtSn/$CeO_2$–C electrocatalyst have a more defined hydrogen adsorption–desorption region than PtSn/C. The charge associated to the double layer for PtSn/$CeO_2$–C was similar to that observed for PtSn/C. This implies that the true active areas of the electrodes are nearly the same, which agrees with the similarity of the particle sizes evaluated from XRD measurements using the Scherrer equation [14]. The two peaks observed around 0.8 V and 1.1 V in the cathodic scan may be attributed to the reduction of PtO, $SnO_2$ and $CeO_2$ species.

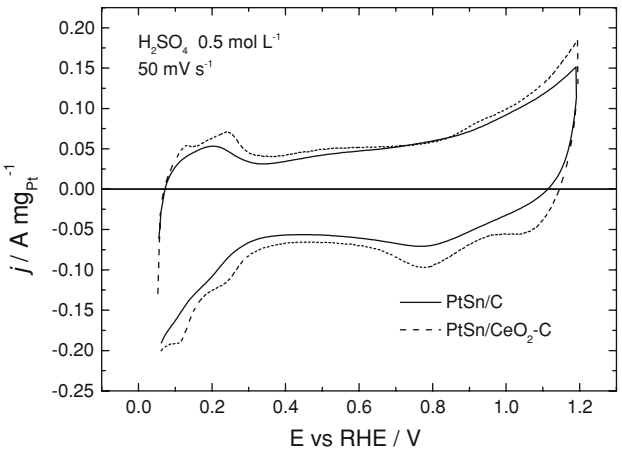


**Fig. 1** Cyclic voltammograms of PtSn/C and PtSn/$CeO_2$–C electrocatalysts in 0.5 mol $L^{-1}$ $H_2SO_4$, sweep rate: 50 mV $s^{-1}$

The PtSn/C and PtSn/$CeO_2$–C electrocatalyst performance in ethanol oxidation are shown in Fig. 2. Ethanol electro-oxidation started at around 0.3–0.4 V for both electrocatalysts; however, at higher potential values PtSn/$CeO_2$–C electrocatalyst showed higher current values than PtSn/C. Thus, a dramatic increase in performance was

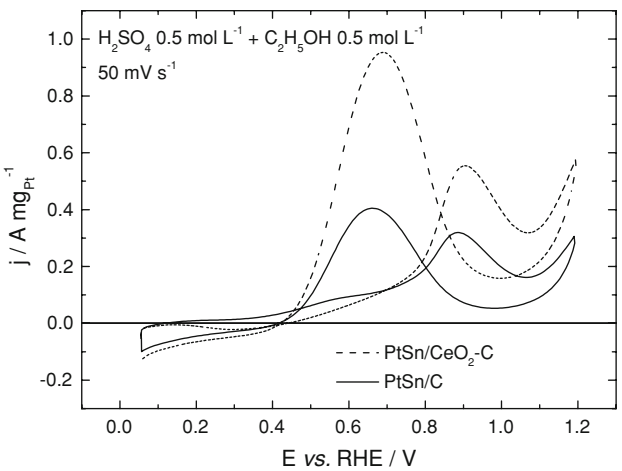


**Fig. 2** Cyclic voltammograms of PtSn/C and PtSn/$CeO_2$–C electrocatalysts in 0.5 mol $L^{-1}$ $H_2SO_4$ solution containing 0.5 mol $L^{-1}$ of ethanol, sweep rate: 50 mV $s^{-1}$

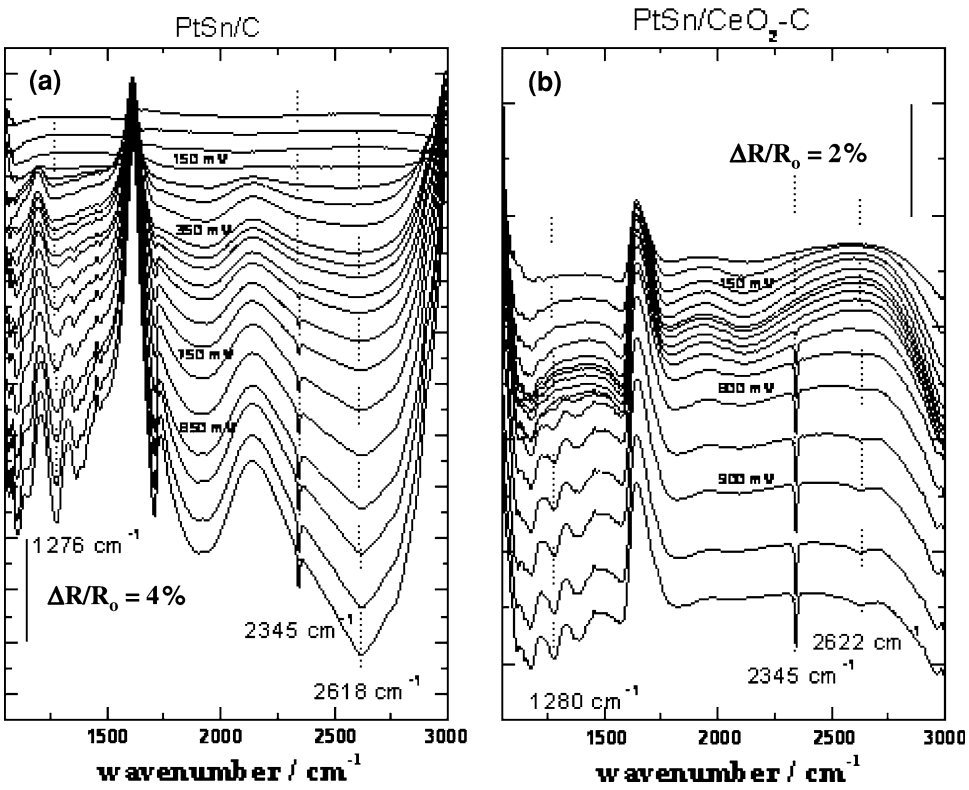


**Fig. 3** In situ FTIR spectra of the species resulting from the oxidation of ethanol in 0.5 mol $L^{-1}$ $H_2SO_4$ + 0.5 mol $L^{-1}$ ethanol on **a** PtSn/C and **b** PtSn/$CeO_2$–C electrocatalysts at potentials varying from 0.100 to 1.000 V vs. RHE. $R_{ERef}$ taken at 0.050 V

obtained with the addition of $CeO_2$. Similar results were observed by Wang et al. [17] on methanol oxidation using PtRu/C catalyst with a loading of 15 wt% of $CeO_2$.

In order to obtain information about intermediates and reaction products in situ infrared spectroscopy was performed in a 0.5 mol $L^{-1}$ $H_2SO_4$ solution containing 0.5 mol $L^{-1}$ $C_2H_5OH$. Figure 3 shows the spectra for PtSn/$CeO_2$-C and PtSn/C in the 1,000–3,000 $cm^{-1}$ spectral range from 0.100 to 1.000 V vs. RHE. These spectra were accumulated at every 50 mV during a cyclic voltammetric experiment run at 1 mV $s^{-1}$. The reference reflectivity used for the calculation of ΔR/R was taken at 0.050 V vs. RHE. The principal bands of the species from ethanol adsorption and oxidation observed in the FTIR spectra may be assigned [18–20]: an absorption band located close to 2,345 $cm^{-1}$ reveals the formation of $CO_2$ species. An absorption band close to 1,725 $cm^{-1}$ attributed to the stretching mode of the carbonyl group (C=O) of acetic acid and/or acetaldehyde coming from the ethanol oxidation. In this case it is difficult to distinguish between the adsorbed carbonyl species from acetic acid or acetaldehyde because C=O bands in these compounds are very close. A broad band located close to 2,600 $cm^{-1}$ that was assigned to the C–H vibration mode of acetic acid or to the OH stretching mode of the carboxylic group overlapped with the C–H stretching mode of the methyl group. The bands close to 1,390 and 1,270 $cm^{-1}$ are attributable to the C–O stretch and O–H deformation vibrations in acetic acid while the bands close to 1,370 and 1,100 $cm^{-1}$ are due to $CH_3$ symmetric deformation and C–H wagging vibration in acetaldehyde and acetic acid.

The FTIR spectra recorded for in situ ethanol oxidation on PtSn/C (Fig. 3a) showed a band at 2,340 $cm^{-1}$ (due to $CO_2$ formation) that was detected from 0.500 to 1.000 V and its intensity increased with increase in potential. A broad band at 2,600 $cm^{-1}$ and the absorption band at 1,270 $cm^{-1}$ (attributed to acetic acid formation) were also detected at potentials higher than 0.450 V and their intensities increased with increase in potential. The absorption band close to 1,725 $cm^{-1}$ (expected for acetaldehyde and/or acetic acid formation) was detected from 0.300–0.350 V and its intensity also increased with increase in potential. It can be also observed that acetaldehyde and/or acetic acid were formed preferentially to $CO_2$. The complete electro-oxidation of ethanol to $CO_2$ releases 12 electrons per molecule, while the partial oxidation to acetaldehyde and acetic acid releases only two and four electrons per molecule, respectively.

The FTIR spectra obtained for the ethanol oxidation on PtSn/$CeO_2$–C electrode (Fig. 3b) showed that the band at 2,340 $cm^{-1}$ (due to $CO_2$ formation) and the bands at 2,600 and 1,270 $cm^{-1}$ (associated to acetic acid formation) were detected in the potential range from 0.500 to 1.000 V. A surprising observation was the non clear observation of the band at 1,725 $cm^{-1}$ in the spectra (attributed to the formation of acetaldehyde and/or acetic acid) at all potentials.

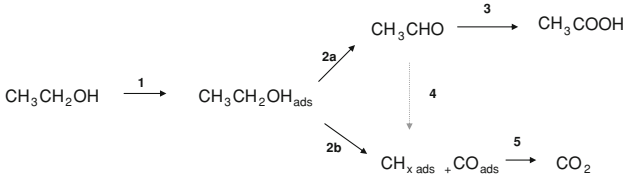


**Scheme 1** Scheme of ethanol oxidation on Pt–Sn electrocatalysts

The above observations infer that $CO_2$ and acetic acid are the main final products formed on $PtSn/CeO_2$–C.

These results suggest that on PtSn/C electrocatalyst the ethanol molecule is initially adsorbed on the Pt surface (step 1) followed by two possible mechanistic routes (see Scheme 1). Thus, α-C–H bond breaking and simultaneous molecular rearrangement occurs to form acetaldehyde (step 2a). The adsorbed acetaldehyde can be desorbed to the solution or it can be further oxidized to acetic acid (step 3). This step occurs through the bifunctional mechanism where the $SnO_2$ provides oxygenated species in order to oxidize acetaldehyde into acetic acid. On $PtSn/CeO_2$–C electrocatalyst the formation of acetic acid may be explained by the same route (step 1, 2a and 3); however, the result regarding the absence of the band at 1,725 $cm^{-1}$ in the spectra, suggests that as soon as the acetaldehyde was formed it was rapidly transformed into acetic acid. In this case, the bifunctional mechanism is favored by the beneficial synergistic effect of $SnO_2$ and $CeO_2$, since cerium oxide is well known in heterogeneous catalysis as a good source of oxygenated species [21]. Experiments to verify this last supposition are currently in progress. The formation of $CO_2$ species may be explained by C–C bond breaking of the adsorbed acetaldehyde molecule (step 4) as soon as it is formed, leading to the formation of two intermediate adsorbed species, CO and a $CH_x$ fragment, that are further oxidized to $CO_2$ (step 5). The formation of $CO_2$ as product may also occur by C–C bond breaking of the adsorbed ethanol (steps 1, 2b and 5).

## 4 Conclusions

$PtSn/CeO_2$–C electrocatalysts prepared by an alcohol-reduction process exhibited higher performance for ethanol oxidation than PtSn/C electrocatalyst. FTIR studies for ethanol oxidation on PtSn/C electrocatalyst showed that acetaldehyde and acetic acid were the principal products formed. On $PtSn/CeO_2$–C the principal final products formed were $CO_2$ and acetic acid. This delivers more electrons per ethanol molecule and explains the highest voltammetric current values obtained for this catalyst. Thus, the addition of $CeO_2$ to PtSn/C electrocatalyst leads to a more complete oxidation of the ethanol molecule. These features should be investigated using other in situ techniques to identify the mechanisms occurring. Also, experiments using these electrocatalysts in real conditions (single direct ethanol fuel cell) and the identification of the products formed under these conditions are currently in progress.

**Acknowledgments** The authors thank FINEP-Pro$H_2$, CNPq, and FAPESP for financial support.

## References

1. Lamy C, Lima A, Lerhum V, Delime F, Coutanceau C, Léger JM (2002) J Power Sources 105:283
2. Wendt H, Spinacé EV, Neto AO, Linardi M (2005) Quim Nova 28:1066
3. Vigier F, Coutanceau C, Perrard A, Belgsir EM, Lamy C (2004) J Appl Electrochem 34:439
4. Antolini E (2007) J Power Sources 170:1
5. Song S, Tsiakaras P (2006) Appl Catal B 63:187
6. Wang H, Jusys Z, Behm RJ (2006) J Power Sources 154:351
7. Rousseau S, Countanceau C, Lamy C, Léger JM (2006) J Power Sources 158:18
8. Zhou WJ, Zhou B, Li WZ, Zhou ZH, Song SQ, Sun GQ, Xin Q, Douvartzides S, Goula M, Tsiakaras P (2004) J Power Sources 126:16
9. Lamy C, Rousseau S, Belgsir EM, Coutanceau C, Léger JM (2004) Electrochim Acta 49:3901
10. Zhou W, Zhou Z, Song S, Li W, Sun G, Tsiakaras P, Xin Q (2003) Appl Catal B 46:273
11. Spinacé EV, do Vale LAI, Dias RR, Neto AO, Linardi M (2006) Stud Surf Sci Catal 162:617
12. Neto AO, Dias RR, Tusi MM, Linardi M, Spinacé EV (2007) J Power Sources 166:87
13. Mann J, Yao N, Bocarsly A (2006) Langmuir 22:10432
14. Neto AO, Farias LA, Dias RR, Brandalise M, Linardi M, Spinacé EV (2008) Electrochem Commun 10:1315
15. Spinacé EV, Neto AO, Vasconcelos TRR, Linardi M (2004) J Power Sources 137:17
16. Spinacé EV, Neto AO, Vasconcelos TRR, Linardi M (2003). Patent BR200304121-A
17. Wang KW, Huang SY, Yeh CT (2007) J Phys Chem C 111:5096
18. Vigier F, Rousseau S, Coutanceau C, Leger JM, Lamy (2006) C Top Catal 40:111
19. Wang Q, Sun GQ, Jiang LH, Xin Q, Sun SG, Jiang YX, Chen SP, Jusys Z, Behm RJ (2007) Phys Chem Chem Phys 9:2686
20. Ribeiro J, dos Anjos DM, Kokoh KB, Coutanceau C, Leger JM, Olivi P, de Andrade AR, Tremiliosi-Filho G (2007) Electrochim Acta 52:6997
21. Machida M, Murata Y, Kishikawa K, Zhang D, Ikeue K (2008) Chem Mater 20:4489